Real-time Implementation of a Novel Safety Function for Prevention of Loss of Vehicle Control

Real-time Implementation of a Novel Safety Function for Prevention of Loss of Vehicle Control

Mohammad Ali[a,b], Claes Olsson[a] and Jonas Sjöberg[b]

***Abstract*— We present a novel safety function for prevention of vehicle control loss. The safety function overcomes some of the limitations of conventional Electronic Stability Control (ESC) systems. Based on sensor information about the host vehicle's state and the road ahead, a threat assessment algorithm predicts the future evolution of the vehicle's state. If the vehicle motion, predicted over a finite time horizon violates safety constraints, autonomous deceleration is activated in order to prevent vehicle loss of control. The safety function has been implemented in real-time. Experimental results indicate that the safety function relies less on the driver's skills than conventional ESC systems and that a more controllable and comfortable vehicle motion can be acquired when the function is active.**

***Index Terms*— Vehicle Stability, Semi-Autonomous Vehicles, Threat Assessment, Active Safety.**

I. Introduction

Roadway departure related crashes account for a great share of all traffic related accidents. According to [13], in developed countries about half of all fatal and a third of all severe vehicle accidents are due to single vehicle crashes. Over the last three decades, several research and technological advancements have contributed to the reduction of fatal roadway departures. Probably the first milestone in active safety dates back to the seventies, when Antilock Braking Systems (ABS) were put into production in passenger cars [4]. Successively, in the mid-1990s, car manufacturers began to equip vehicles with Electronic Stability Control (ESC) systems which have proven to be efficient in reducing the amount of fatal roadway departures that are caused by loss of vehicle control. Studies have shown that ESC systems reduce the amount of fatal single vehicle crashes by 30-50% for cars and 50-70% for Sport Utility Vehicles (SUVs) [7].

A drastic increase of the overall vehicle safety is expected from future active safety systems, which are envisioned to rely on sophisticated sensing infrastructures providing preview of the coming road and information about the surrounding environment. Such preview capabilities are expected to enable early interventions, in order to prevent vehicles from working in unsafe operating conditions where classical active safety systems like ESC are activated. Moreover, the possibility of partially or completely replacing the driver with an autonomous driving system will enable the ability to recover vehicle control in critical scenarios, where the coordination of multiple vehicle actuators might lead to more effective evasive maneuvers.

[a]*Active Safety and Chassis, Volvo Car Corporation, PV4A/96410, 405 31 Göteborg, Sweden.*

[b]*Department of Signals and Systems, Chalmers University of Technology, SE-412 96 Göteborg, Sweden*

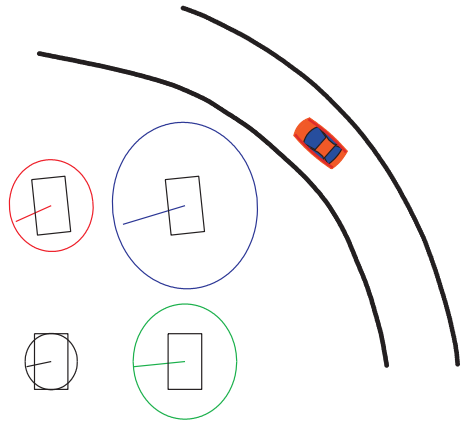

Fig. 1. Illustration of a vehicle's vertical load distribution in a curve situation. The ellipses are so called friction ellipses and represent available friction at each of the four wheels. The size of each ellipse depends on the vertical load at that wheel. The force vector produced at the contact patch of each wheel is constrained to lye within the friction ellipse at that wheel. In a curve situation, much of the vehicle's weight is redistributed to the outer side, hence available brake force at the inner back wheel is greatly reduced.

In this paper we address some of the limitations of conventional ESC systems which are not ready to take advantage of preview capabilities envisioned to be a standard functionality in future vehicles. Rather than utilizing knowledge about the coming road, conventional ESC systems rely heavily on the driver's actions when controlling the vehicle's motion. Based on the steering wheel angle provided by the driver, ESC systems compute a desired trajectory, which is tracked in order to maintain safe travel. By commanding a desired trajectory, a skilled driver can efficiently utilize the ESC system in extremely challenging situations to keep the vehicle on the road. Normal or unexperienced drivers however, might panic in such situations and fail to guide the ESC system in order to maintain a safe trajectory. In fact, according to [17], it is common that vehicle motion reaches the limit of adhesion between tire and road due to the panic reactions of the driver.

Another limitation with conventional ESC systems is that loss of vehicle control is detected only once it has already occurred. Consider Figure 1, which illustrates a situation where a vehicle is negotiating a curve. Due to excessive speed, the vehicle's yaw rate is too low to follow the curvature of the road and the driver is incapable of generating enough yaw moment through steering only. In this situation, a conventional ESC system would typically brake the inner rear wheel of the vehicle in order to generate a yaw moment which would in turn increase the yaw rate

of the vehicle in the desired direction. Due to the vehicle's lateral acceleration a large portion of the vehicle's weight is however redistributed to the outer side of the vehicle in such a situation. The available friction at each tire depends on the normal force acting on the tire, hence a small vertical load at the inner rear wheel also means that available friction at that wheel is low. The influence of the brake intervention is thus limited and if the situation is severe, available brake force is not sufficient to keep the vehicle on the road. If an intervention would be issued earlier, before available friction is reduced at the inner rear wheel a more significant effect would be acquired, thus increasing the possibility for the vehicle to stay on the road.

In this work, we assume the availability of advanced sensing systems, providing preview of the road geometry. We propose a novel active safety function which, based on preview information, prevents the vehicle from operating in conditions where assistance from an ESC system is normally needed.

II. Modeling

In this section, we present the mathematical models used in the threat assessment and control design to account for the vehicle behavior.

A. Vehicle model

Consider the notation introduced in Figure 2. We use the following set of differential equations to describe the vehicle motion within the lane,

$$m\dot{v}_x = mv_y\dot{\psi} + \sum_{i=1}^{4} F_{xi}, \tag{1a}$$

$$m\dot{v}_y = -mv_x\dot{\psi} + \sum_{i=1}^{4} F_{yi}, \tag{1b}$$

$$J_z\ddot{\psi} = l_f(F_{y1}+F_{y2}) - l_r(F_{y3}+F_{y4}) + \frac{w_t}{2}(-F_{x1}+F_{x2}-F_{x3}+F_{x4}), \tag{1c}$$

$$\dot{e}_\psi = \dot{\psi} - \dot{\psi}_d, \tag{1d}$$

$$\dot{e}_y = v_y\cos(e_\psi) + v_x\sin(e_\psi), \tag{1e}$$

where, m and J_z denote the vehicle mass and yaw inertia, respectively, l_f and l_r denote the distances from the vehicle center of gravity to the front and rear axles respectively and w_t denotes the track width. v_x and v_y denote the vehicle longitudinal and lateral velocities, respectively, $\dot{\psi}$ is the turning rate around a vertical axis at the vehicle's center of gravity. e_ψ and e_y in Figure 2 denote the vehicle orientation and lateral position, respectively, in a road aligned coordinate system and ψ_d is the desired vehicle orientation, i.e., the slope of the tangent to the curve Γ_d in the point O. F_{xi} and F_{yi} are tire forces acting along the longitudinal and lateral vehicle axis, respectively.

Forces are generated at the contact patch between tire and road. We denote by f_{xi} and f_{yi} the force components acting along the longitudinal and lateral tire axis, which lead to the following longitudinal and lateral forces in the vehicle body frame,

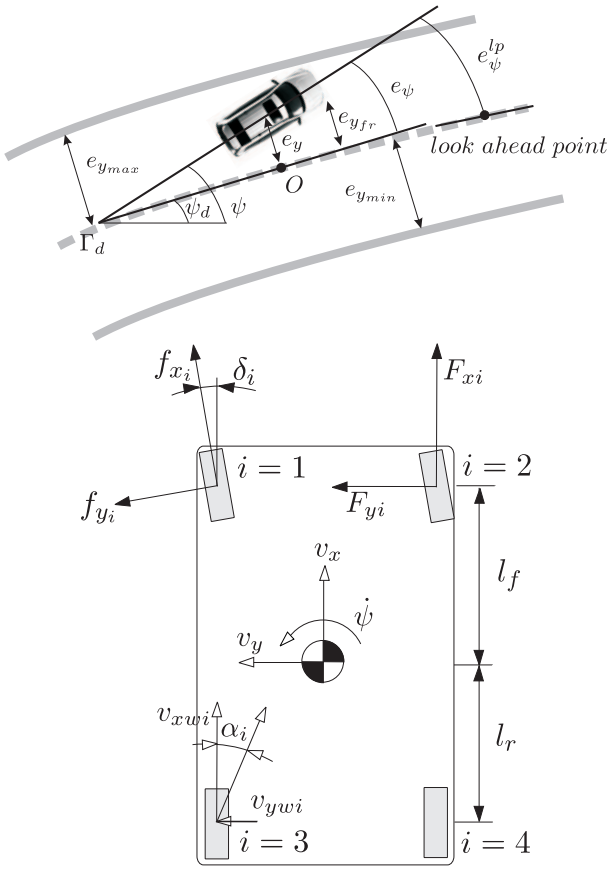

Fig. 2. Modeling notation.

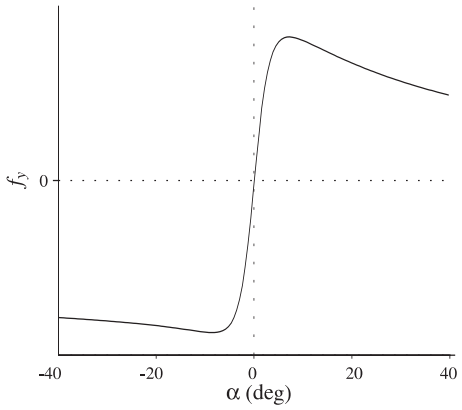

Fig. 3. Lateral tire force characteristics.

$$F_{xi} = f_{xi}\cos(\delta_i) - f_{yi}\sin(\delta_i), \tag{2a}$$

$$F_{yi} = f_{xi}\sin(\delta_i) + f_{yi}\cos(\delta_i), \qquad i \in \{1,2,3,4\}. \tag{2b}$$

The lateral tire forces f_{yi} are computed using a simplified version of the well known Pacejka magic tire formula [10],

$$f_{y_i} = \mu_i F_{z_i}\sin\left(C_i\arctan\left(B_i\alpha_i\right)\right), \tag{3}$$

where μ_i denotes the road friction coefficient, F_{zi} denotes the vertical load and C_i, B_i are tire parameters that are calibrated

using experimental data. The lateral tire slip angle α in (3) is illustrated in Figure 2 and is defined as the angle between the velocity vector of the wheel and the wheel's direction, i.e.,

$$\alpha_i = \arctan \frac{-v_{ywi}}{v_{xwi}}, \tag{4}$$

where $v_{xwi},\ v_{ywi}$ are the longitudinal and lateral components of the wheel's velocity at wheel i, respectively. Figure 3 illustrates the lateral tire force characteristics (3). The velocity components v_{xwi} and v_{ywi} in equation (4) are computed as,

$$v_{xw1} = (v_y + l_f\dot{\psi})\sin\delta_1 + (v_x - \frac{w_t}{2}\dot{\psi})\cos\delta_1, \tag{5a}$$

$$v_{yw1} = (v_y + l_f\dot{\psi})\cos\delta_1 - (v_x - \frac{w_t}{2}\dot{\psi})\sin\delta_1, \tag{5b}$$

$$v_{xw2} = (v_y + l_f\dot{\psi})\sin\delta_2 + (v_x + \frac{w_t}{2}\dot{\psi})\cos\delta_2, \tag{5c}$$

$$v_{yw2} = (v_y + l_f\dot{\psi})\cos\delta_2 - (v_x + \frac{w_t}{2}\dot{\psi})\sin\delta_2, \tag{5d}$$

$$v_{xw3} = (v_y - l_r\dot{\psi})\sin\delta_3 + (v_x - \frac{w_t}{2}\dot{\psi})\cos\delta_3, \tag{5e}$$

$$v_{yw3} = (v_y - l_r\dot{\psi})\cos\delta_3 - (v_x - \frac{w_t}{2}\dot{\psi})\sin\delta_3, \tag{5f}$$

$$v_{xw4} = (v_y - l_r\dot{\psi})\sin\delta_4 + (v_x + \frac{w_t}{2}\dot{\psi})\cos\delta_4, \tag{5g}$$

$$v_{yw4} = (v_y - l_r\dot{\psi})\cos\delta_4 - (v_x + \frac{w_t}{2}\dot{\psi})\sin\delta_4. \tag{5h}$$

We make use of the following assumptions,

Assumption 1: In equation (3) the vertical forces F_{zi} are assumed constant and determined by the vehicle's steady state weight distribution when no lateral or longitudinal forces act on the vehicle.

Assumption 2: The friction coefficient enters the system equations as a disturbance, is assumed to be the same at all wheels i.e. $\mu_i = \mu,\ \forall i$ and constant over a finite time horizon. At each time instant an estimate of μ is assumed available, see e.g. [18], [14], [11], [16] for friction estimation techniques.

Assumption 3: The signal $\dot{\psi}_d$ in (1d) enters the system equations as a disturbance. Every time instant, an estimate of the disturbance $\dot{\psi}_d$ is avilable over a finite time horizon. Estimates of this disturbance signal can be obtained on-line by using the measurement setups used in [9], [1], [5].

Assumption 4: $\delta_1 = \delta_2 = \delta$ and $\delta_3 = \delta_4 = 0$.

Assumption 5: We assume $v_{xwi} \approx v_x + (-1)^i \frac{w_t}{2}\dot{\psi}$ and approximate the slip angles as,

$$\alpha_1 = \frac{v_y + l_f\dot{\psi}}{v_x - \frac{w_t}{2}\dot{\psi}} - \delta, \qquad \alpha_2 = \frac{v_y + l_f\dot{\psi}}{v_x + \frac{w_t}{2}\dot{\psi}} - \delta, \tag{6a}$$

$$\alpha_3 = \frac{v_y - l_r\dot{\psi}}{v_x - \frac{w_t}{2}\dot{\psi}}, \qquad \alpha_4 = \frac{v_y - l_r\dot{\psi}}{v_x + \frac{w_t}{2}\dot{\psi}}. \tag{6b}$$

The vehicle model (1)-(6) is written in the following compact form,

$$\dot{\varkappa}(t) = f_{veh}(\varkappa(t), u(t), w(t)) \tag{7}$$

where $\varkappa = \begin{bmatrix} v_x,\ v_y,\ \dot{\psi},\ e_\psi,\ e_y \end{bmatrix}^T$ is the state vector, $u = [\delta,\ f_{x1},\ f_{x2},\ f_{x3},\ f_{x4}]^T$ the input vector and $w = \begin{bmatrix} \mu,\ \dot{\psi}_d \end{bmatrix}^T$ is the disturbance vector.

B. Linear single track vehicle model

For the threat assessment presented in Section III, we will also consider a linear single track vehicle model. In this case we will only consider the lateral and yaw dynamics in the vehicle body frame. Compared to the model (7), the following simplifications are used,

Simplification 1: The track width is set to zero and the left and right wheels at each axle are lumped together. The tire slip angle at the front and rear axles are then obtained by setting $w_t = 0$ in (6a) and (6b), respectively.

Simplification 2: The lateral tire force is approximated as linearly related to the tire slip angle,

$$f_{yj} = (B_j C_j \mu F_{zj})\alpha_j, \quad j \in \{f, r\}, \tag{8}$$

where the subscripts $(\cdot)_f, (\cdot)_r$ are used to particularize variables at the front and rear axles respectively.

Remark 1: The linear tire model (8) approximates, the more complex nonlinear tire characteristics well only when restricting the vehicle operation to limited values of α, see Figure 3. This is also a region of the state space where normal drivers are used to operate and feel comfortable in maneuvering the vehicle [10], [8].

This results in a two-degrees of freedom linear model which can be compactly written as,

$$\dot{\xi}(t) = A\xi(t) + B\delta(t), \tag{9}$$

where $\xi = \begin{bmatrix} v_y,\ \dot{\psi} \end{bmatrix}^T$ is the state vector. The matrices $A,\ B$ follow immediately from the equations above.

C. Driver model

In this paper the driver is described through a model, where the vehicle's state and the environment information are exogenous signals. In general, the model can range from the very simple structure used in this paper to complex model structures accounting for a large amount of exogenous signals [2]. For instance, the model could be a hybrid model, where different driver dynamics are selected depending on the vehicle operating regions and drowsiness estimated through, e.g., driver monitoring cameras inside the vehicle. In our study we are interested in very simple model structures, enabling the design of a low complexity model-based threat assessment algorithm.

Define the orientation error e_ψ^{lp}, w.r.t. the look-ahead point in Figure 2, as

$$e_\psi^{lp} = \psi - \psi_d^{lp} = e_\psi + \Delta\psi_d, \tag{10}$$

where ψ_d^{lp} is the desired orientation at time $t + t_{lp}$, with t the current time, $\Delta\psi_d = \psi_d - \psi_d^{lp}$ and t_{lp} the preview time that can be mapped into the preview distance d_{lp} under the assumption of constant speed v_x. We compute the steering angle δ as

$$\delta = K_y e_y + K_\psi e_\psi^{lp} = K_y e_y + K_\psi e_\psi + K_\psi \Delta\psi_d, \tag{11}$$

with $K_y,\ K_\psi$ gains that are, in general, time varying and might be updated online.

Clearly, $\Delta\psi_d$ in (10) depends on the preview time t_{lp} that, in our modeling framework, is considered as a parameter of the driver model and can be identified from experimental data. Recursive least squares estimation results of the driver's model parameters are demonstrated in [6].

The driver model considered here does not apply any longitudinal force which leads to the following control law,

$$u(t) = \begin{bmatrix} \mathbf{0}_{1\times 3} & [K_\psi \ K_y] \\ \mathbf{0}_{4\times 3} & \mathbf{0}_{4\times 2} \end{bmatrix} \varkappa(t) + \begin{bmatrix} K_\psi \Delta\psi_d(t) \\ \mathbf{0}_{4\times 1} \end{bmatrix}. \quad (12)$$

III. Predictive control loss prevention

In this section we describe the safety function, Predictive Control Loss Prevention (PCLP), proposed in this paper. The threat assessment module, which repeatedly evaluates the threat level is described in Section III-A, while the intervention activated once an increased threat is detected is described in Section III-B.

A. Threat assessment

Consider the autonomous system, obtained by combining the vehicle models (7) and (9) with the control law (12),

$$\dot{x}(t) = f_a(x(t), w(t)), \quad (13)$$

where $x = \begin{bmatrix} \varkappa^T, \ \xi^T \end{bmatrix}^T$. We discretize the model (13) with a sampling time T_s,

$$x(t+1) = f_a^{DT}(x(t), w(t)), \quad (14)$$

where, with an abuse of notation, the same symbols are used to denote the time, state and exogenous signal vectors of the system (13) and its discrete time version (14).

Denote by $\mathbb{X}\left(t, x(t), \mathcal{W}_{[t,t+H_T-1]}\right) = [x_{t,t}, \ldots, x_{t+H_T-1,t}]$, where $\mathcal{W}_{[t,t+H_T-1]} = [w(t), \ldots, w(t+H_T-1)]$, a state trajectory over the time interval $[t, \ldots, t+H_T-1]$ obtained as a solution to the, in general nonlinear, differences equation (14), with initial condition $x_{t,t} = \left[\varkappa^T(t), \xi^T(t)\right]^T$.

We let,

$$\Omega_{t+l,t} = [0, 0, 1, 0, 0, 0, -1] x_{t+l,t}, \quad (15)$$

denote the difference between the yaw rate predicted by the nonlinear vehicle model (7) and by the linear vehicle model (9) at time $t+l$, with $x_{t,t} = x(t)$. The difference between a vehicle's yaw rate and a *nominal* yaw rate computed through a simplified linear vehicle model is often used in electronic stability control systems to activate closed loop control of the vehicle motion and is also regulated to zero once the motion control has been activated [15], [17], [12]. The predicted output is defined as,

$$y_{t+l,t} = h(x_{t+l,t}) = [\Omega_{t+l,t}, \ \alpha_{1_{t+l,t}}, \ \alpha_{2_{t+l,t}}, \ \alpha_{3_{t+l,t}}, \ \alpha_{4_{t+l,t}}]^T, \quad (16)$$

where $\alpha_{i_{t+l,t}}$, denotes predicted tire slip angles computed using the relation (6). The following safety constraints are introduced,

$$-y_{bound} \leq y_{t+l,t} \leq y_{bound}, \quad l \in \{0, \ldots, H_T - 1\}. \quad (17)$$

This is a region of the state space where a normal driver is deemed capable of maintaining a stable vehicle motion, see Remark 1.

We introduce a threat assessment function $\mathbb{T}\left(\mathbb{X}\left(t, x(t), \mathcal{W}_{[t,t+H_T-1]}\right)\right)$. The definition of the function $\mathbb{T}$ is crucial in the considered accident avoidance function. In particular, $\mathbb{T}$ can range from a simple time invariant function, e.g., evaluating the distance of the vehicle from the road centerline, to a complex time varying function detecting the collision with moving objects. In our predictive control loss prevention function we let $\mathbb{Y} = [y_{t,t}, \ldots, y_{t+H_T,t}]^T$, $\mathbb{Y}_{bound} = [y_{bound}, \ldots, y_{bound}]^T$, where $\mathbb{Y}$ and $\mathbb{Y}_{bound}$ have the same dimension and define the threat assessment function as,

$$\mathbb{T}(\mathbb{X}) = \begin{bmatrix} \mathbb{Y} \\ -\mathbb{Y} \end{bmatrix} - \begin{bmatrix} \mathbb{Y}_{bound} \\ \mathbb{Y}_{bound} \end{bmatrix}. \quad (18)$$

Components of $\mathbb{T}$ are positive if the vehicle motion, predicted over a time horizon of H_T steps, through the autonomous system model (14), violates safety constraints, less than or equal to zero otherwise.

B. Autonomous deceleration

If any component of $\mathbb{T}$ in (18) is positive at time t, the vehicle is expected to evolve to a region of the state space where a normal driver's ability to maneuver the vehicle is reduced (Remark 1). An intervention is then activated to autonomously decelerate the vehicle with an acceleration a_{dec} while the steering is left to the driver. Many vehicles today are already equipped with cruise control and/or collision avoidance systems [3]. To achieve a certain acceleration level these systems commonly rely on lower level controllers that control the torque applied to the wheels based on an acceleration request a_{req}. We assume the availability of such a lower level controller.

C. Main Algorithm

The main steps underlying the present safety function are outlined in Algorithm 1. We note that in Steps 4 and 6 of Algorithm 1 an acceleration request a_{req} is set. We remark however that the driver always has the possibility to use the brake pedal in order to decelerate the vehicle even further.

Algorithm 1 Evaluates whether an intervention is required at each time step and signals a deceleration request if needed.

Input: Current state measurement $x(t)$, sequence of disturbances $\mathcal{W}_{[t,t+H_T-1]}$, state update function f_a^{DT}, output map h, output bounds $\mathbb{Y}_{bound}$.

Output: Acceleration request a_{req}

1: Compute $\mathbb{X}\left(t, x(t), \mathcal{W}_{[t,t+H_T-1]}\right)$
2: Evaluate $\mathbb{T}(\mathbb{X})$
3: **if** $\mathbb{T}(\mathbb{X}) \leq 0$ **then**
4: $\quad a_{req} = a_b$
5: **else**
6: $\quad a_{req} = 0$
7: **end if**
8: **return** a_{req}

IV. Results

The suggested safety function PCLP has been implemented in a rapid prototyping system and tested in real-time on both high- and low-friction surfaces with promising results. The low-friction surface tests where conducted at a frozen lake in the north of Sweden. Due to the absence of lane markings on the lake, a digital map of the ice-track was recorded to obtain the road geometry. Each vehicle position on the track, provided by a differential GPS-system, could then be mapped to e.g. a corresponding lane-width and curvature. In the low-friction surface tests, the friction coefficient was manually set to $\mu = 0,25$. In addition the experimental vehicle was equipped with an ESC system and a collision avoidance system. The vehicle's interface to the collision avoidance system was used to command the autonomous deceleration interventions in the experimental tests.

For the sake of brevity we will only show low-friction surface test results in this paper. Consider the four velocity trajectories reported in Figure 4. The trajectories where

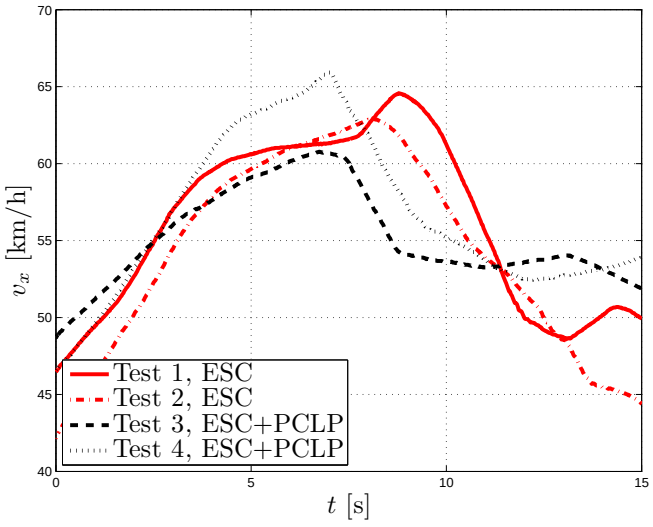

Fig. 4. Longitudinal velocity

collected by driving four times through the same curve and trying to approach the curve with the same velocity each time. In the Tests 1 and 2, the driver is only assisted by the conventional ESC system while in the Tests 3 and 4, the suggested safety function PCLP has also been activated.

We observe that in the four tests, the vehicle was accelerating slightly as approaching the curve. PCLP activated a braking intervention at approximately the same point in the tests 3 and 4 and the braking was stopped at approximately the same velocity in both cases. In the tests 1 and 2 on the other hand, the vehicle was allowed to keep accelerating into the curve until an ESC intervention was activated. We note that, even though the ESC system only brakes individual wheels, a larger velocity reduction is obtained in this case as a consequence of the control loss.

Figure 5 shows the vehicle's path in the four tests. We

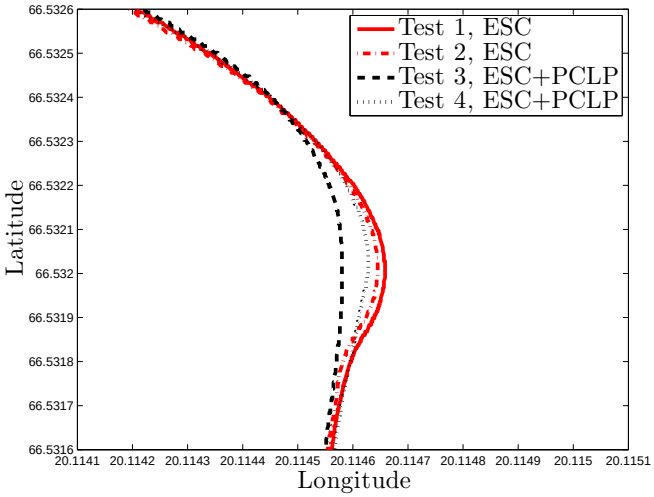

Fig. 5. Vehicle position

observe that, without PCLP the vehicle is required to take a wider path.

In Figure 6 the vehicle's yaw rate is plotted. In the Tests 1

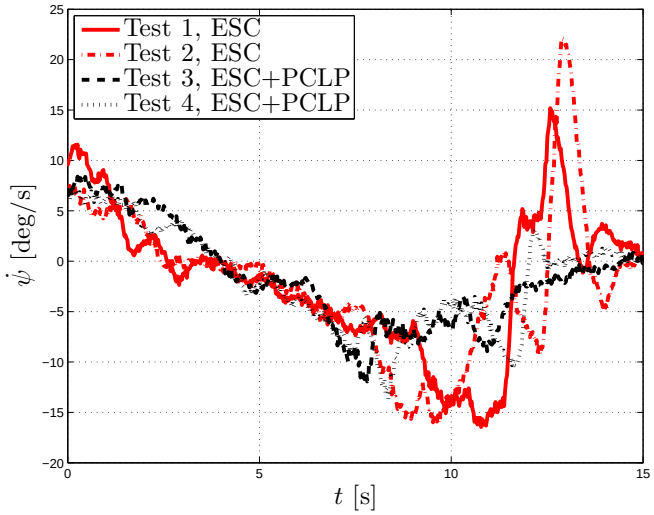

Fig. 6. Yaw rate

and 2 we observe a higher yaw rate in the beginning of the curve when compared to Tests 3 and 4. We also note that in order to recover the vehicle's orientation a high yaw rate in the opposite direction is acquired in the Tests 1 and 2. This is also seen in the steering angle plotted in Figure 7. In order to follow the road geometry, the driver is required to steer more when only ESC is activated and later needs to countersteer in order to recover the vehicle's intended path. We emphasize that these tests were performed by an expert driver and that not all drivers are skilled enough to perform such countersteer maneuvers. When PCLP is activated we observe however that due to the initially reduced velocity, the driver's skills are not as critical.

Finally in Figures 8 and 9 we see the vehicle's lateral velocity and acceleration, respectively. A higher magnitude

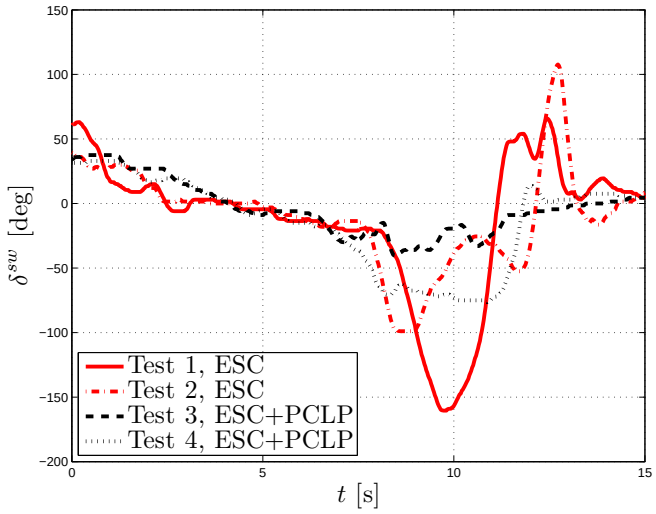

Fig. 7. Steering wheel angle

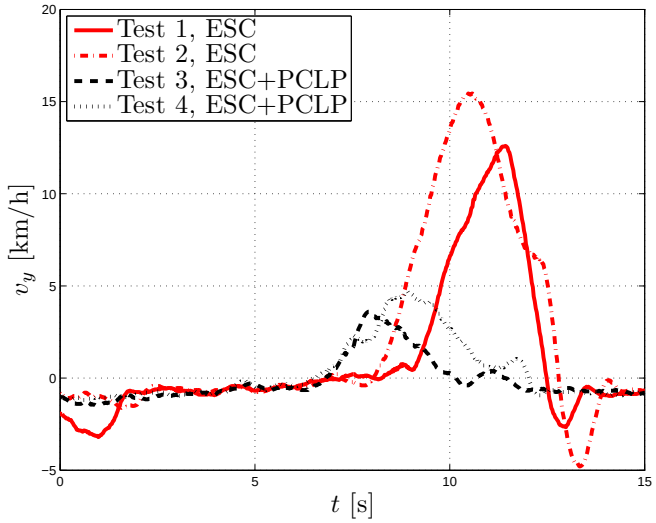

Fig. 8. Lateral velocity

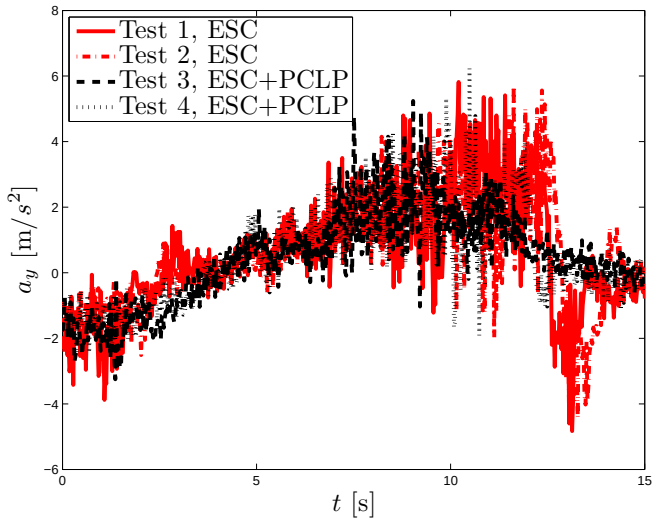

Fig. 9. Lateral acceleration

in both lateral velocity and acceleration is acquired when ESC operates alone, compared to the case with PCLP active. We conclude that a more controllable and convenient motion can be acquired with PCLP.

V. Concluding remarks and future work

We have presented a novel safety function for prevention of vehicle loss of control. The safety function has been implemented in a rapid prototyping system and evaluated in real-time with promising results. Experimental results indicate that the safety function relies less on the driver's skills than conventional ESC systems and that a more controllable and comfortable vehicle motion can be acquired when the function is active. An evaluation of the functions performance and requirements on sensor accuracy is currently being conducted on a large set of logged naturalistic driving data.

References

[1] M Bertozzi, A Broggi, and A Fascioli. Vision-based intelligent vehicles: State of the art and perspectives. *Robotics and Autonomous Systems*, 32(1):1–16, July 2000.

[2] C Cacciabue. *Modelling Driver Behaviour in Automotive Environments*. Springer, 2007.

[3] Martin Distner, Mattias Bengtsson, Thomas Broberg, and Lotta Jakobsson. City Safety A System Addressing Rear-End Collisions at Low Speeds. *In Proc. 21st International Technical Conference on the Enhanced Safety of Vehicles*, 2009.

[4] A. Eidehall. *Tracking and threat assessment for automotive collision avoidance*. PhD thesis, Linköping University, 2007.

[5] A Eidehall, J Pohl, and F Gustafsson. Joint road geometry estimation and vehicle tracking. *Control Engineering Practice*, 2007.

[6] Paolo Falcone, Mohammad Ali, and Sjöberg Jonas. Predictive Threat Assessment via Reachability Analysis and Set Invariance Theory. *Accepted for publication in IEEE Transactions on Intelligent Transportation Systems*, 2011.

[7] S A Ferguson. The Effectiveness of Electronic Stability Control in Reducing Real-World Crashes: A Literature Review. *Traffic Injury Prevention*, 2007.

[8] T D Gillespie. *Fundamentals of Vehicle Dynamics*. Society of Automotive Engineers, Inc, 1992.

[9] J Jansson. *Collision avoidance theory with application to automotive collision mitigation*. PhD thesis, 2005.

[10] H Pacejka. *Tyre and Vehicle Dynamics*. Elsevier Ltd, 2006.

[11] W. R. Pasterkamp and H. B. Pacejka. The Tyre as a Sensor to Estimate Friction. *Vehicle System Dynamics*, 27(5):409–422, June 1997.

[12] R. Rajamani. *Vehicle Dynamics and Control*. Springer, 2006.

[13] J Sandin and M Ljung. Understanding the causation of single-vehicle crashes: a methodology for in- depth on-scene multidisciplinary case studies. *International Journal of Vehicle Safety (IJVS)*, 2007.

[14] T Shim and D Margolis. Model-Based Road Friction Estimation Model-Based Road Friction Estimation. *Vehicle System Dynamics*, 41:249–276, 2004.

[15] H E Tseng, B Ashrafi, D Madau, T A Brown, and D Recker. The Development of Vehicle Stability Control at Ford. *IEEE/ASME Transactions on Mechatronics*, 4, September 1999.

[16] H Tsunashima, M Murakami, and Miyata J. Vehicle and road state estimation using interacting multiple model approach. *Vehicle System Dynamics*, 44, 2006.

[17] A T Van Zanten. Bosch ESP System: 5 Years of Experience. *SAE*, 2000.

[18] S Yamazaki, O Furukawa, and T Suzuki. Study on Real Time Estimation of Tire to Road Friction. *Vehicle System Dynamics*, 27:225–233, 1997.